



UNIVERSITY OF LEEDS

This is a repository copy of *Intracellular Hydrogen Peroxide Detection with Functionalised Nanoelectrodes*.

White Rose Research Online URL for this paper:
<http://eprints.whiterose.ac.uk/103995/>

Version: Accepted Version

Article:

Marquitan, M, Clausmeyer, J, Actis, P orcid.org/0000-0002-7146-1854 et al. (5 more authors) (2016) Intracellular Hydrogen Peroxide Detection with Functionalised Nanoelectrodes. *ChemElectroChem*, 3 (12). pp. 2125-2129. ISSN 2196-0216

<https://doi.org/10.1002/celc.201600390>

© 2016 WILEY-VCH Verlag GmbH & Co. This is the peer reviewed version of the following article: Marquitan, M., Clausmeyer, J., Actis, P., Córdoba, A. L., Korchev, Y., Mark, M. D., Herlitze, S. and Schuhmann, W. (2016), Intracellular Hydrogen Peroxide Detection with Functionalised Nanoelectrodes. *CHEMELECTROCHEM.*; which has been published in final form at <https://dx.doi.org/10.1002/celc.201600390>. This article may be used for non-commercial purposes in accordance with the Wiley Terms and Conditions for Self-Archiving.

Reuse

Unless indicated otherwise, fulltext items are protected by copyright with all rights reserved. The copyright exception in section 29 of the Copyright, Designs and Patents Act 1988 allows the making of a single copy solely for the purpose of non-commercial research or private study within the limits of fair dealing. The publisher or other rights-holder may allow further reproduction and re-use of this version - refer to the White Rose Research Online record for this item. Where records identify the publisher as the copyright holder, users can verify any specific terms of use on the publisher's website.

Takedown

If you consider content in White Rose Research Online to be in breach of UK law, please notify us by emailing eprints@whiterose.ac.uk including the URL of the record and the reason for the withdrawal request.



eprints@whiterose.ac.uk
<https://eprints.whiterose.ac.uk/>

Intracellular Hydrogen Peroxide Detection Using Functionalised Nanoelectrodes

Miriam Marquitan,[a] Jan Clausmeyer,*[a] Paolo Actis,[b,d] Ainara López Córdoba,[b] Yuri Korchev,[b] Melanie D. Mark,[c] Stefan Herlitze[c] and Wolfgang Schuhmann*[a]

[a] M. Marquitan, Dr. J. Clausmeyer, Prof. Dr. W. Schuhmann; Analytical Chemistry - Center for Electrochemical Sciences (CES), Ruhr-Universität Bochum; Universitätsstraße 150, D-44780 Bochum, Germany.

email: jan.clausmeyer@rub.de; wolfgang.schuhmann@rub.de

[b] Dr. P. Actis, Dr. A. López Córdoba, Prof. Dr. Y. Korchev; Department of Medicine; Imperial College London; London W12 0NN, United Kingdom

[c] Dr. M. D. Mark, Prof. Dr. S. Herlitze; Department of General Zoology and Neurobiology; Ruhr-Universität Bochum; Universitätsstraße 150, D-44780 Bochum, Germany

[d] Dr. P. Actis; School of Electronic and Electrical Engineering; University of Leeds; Leeds LS2 9JT, United Kingdom

Abstract:

Hydrogen peroxide (H₂O₂) is one of the most important reactive oxygen species and it is involved in a number of cellular processes ranging from signal transduction to immune-defence and oxidative stress. It is of great interest to intracellularly quantify H₂O₂ to improve the understanding of its role in disease processes. In this study, we present an amperometric nanosensor for the quantification of H₂O₂ at the single-cell level. Deposition of the electrocatalyst Prussian Blue on carbon nanoelectrodes enables the selective H₂O₂ reduction at mild potentials. Because of their small size and needle-type shape, these nanoelectrodes can penetrate the membrane of single living cells causing only minimal perturbation. The nanosensors allow the monitoring of penetration-induced oxidative outbursts as well as the uptake of H₂O₂ from the extracellular environment in single murine macrophages.

Introduction

Reactive oxygen and nitrogen species (ROS, RNS) play a key role in physiological processes such as signalling and cell proliferation.[1] However, overproduction leads to oxidative stress which is related to several pathogenic conditions including cardiovascular, cancer and neurodegenerative diseases.[2,3] Their very short lifetime and spatially restricted abundance complicate the detection of ROS or RNS. To date, selective intracellular non-destructive analysis of ROS or RNS species is not available. Conventional ROS and RNS detection methods are based on fluorescent probes, electron-spin resonance approaches and immunoassays.[4] Although widely used, these methods either study cells post-mortem or require labelling which alters the ROS physiology. Additionally, intracellular ROS quantification remains challenging as the reaction mechanism of fluorophores is often unclear and they lack specificity for one particular target molecule.[5] Due to their small size, amperometric sensors based on ultramicro- or nanoelectrodes provide the necessary spatial and temporal resolution which makes them suitable as alternative probes for measurements in tissues[6] and single-cell analysis.[7] Ultramicroelectrodes were previously used to detect ROS/RNS released from single cells to the extracellular environment after stimulation of an immune response.[8,9] Beyond that, tools for the evaluation of intracellular ROS levels are of high

value to elucidate the impact of ROS species on individual cell fates. Recently, intracellular electrochemical ROS detection using platinumised nanoelectrodes was reported.[10] The applied potential was high enough to oxidise most ROS and RNS but also compounds like uric acid or ascorbic acid, which resulted in a lack of specificity. Besides, the outer glass sheath of several hundred nm was rather large in comparison to a single cell. Carbon nanoelectrodes (CNEs) fabricated by pyrolysis of alkane gas in laser-pulled quartz nanopipettes[11,12] exhibit smaller overall dimensions. CNEs were applied for electrochemical measurements in individual cells with minimal cell disturbance, however with yet unsatisfactory specificity for certain ROS species.[13] More recently, we have reported on the modification of CNEs with Prussian Blue (PB), an excellent catalyst for the selective reduction of hydrogen peroxide.[14] Due to the mild potentials applied for detection, these nanosensors allow selective determination of H₂O₂. In this article, we apply these PB nanosensors for the detection of intracellular H₂O₂ in single living cells.

Results and Discussion

CNEs were fabricated from quartz capillaries by laser pulling and subsequent pyrolysis of butane/propane into the formed nanopipettes. The electrodes typically exhibit a radius between 50 and 200 nm as estimated from their steady-state current in a solution of 5 mM [Ru(NH₃)₆]Cl₃. A tight seal between cell membrane and the nanoelectrode tip is crucial to exclude the detection of extracellular species.[15] Human embryonic kidney (HEK) cells immersed in PBS pH 7.4 containing two different redox mediators were penetrated with unmodified CNEs using the measurement setup depicted in Figure 1 a. The hydrophilic mediator [Ru(NH₃)₆]³⁺ does not permeate through the phospholipid bilayer membrane while in contrast ferrocenemethanol (FcMeOH) crosses the membrane due to its hydrophobic nature.

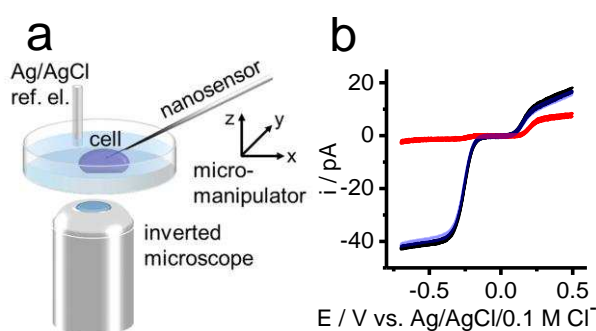


Figure 1. a: Scheme of the experimental setup used for cell penetrations. b: Cyclic voltammograms of a nanoelectrode in 1 mM [Ru(NH₃)₆]Cl₃, 1 mM FcMeOH in PBS pH 7.4, 100 mVs⁻¹. The black and blue line show the cyclic voltammograms in the solution before and after penetration of a HEK cell, respectively. The red line shows the cyclic voltammogram recorded when the nanoelectrode was inserted in a HEK cell.

Cyclic voltammograms were recorded before and after penetration as well as inside of the cytosol (Figure 1 b). After penetration of the CNE into the cell, the redox wave of [Ru(NH₃)₆]Cl₃ is reduced by about 95% while the FcMeOH signal only decreases by approximately 50%. Additionally, an anodic shift of the half-wave potential is observed which is due to the additional contribution of the membrane potential to the external potential applied to the sensor. Together with the absence of the response from the hydrophilic mediator while the hydrophobic one is still detectable, this shift indicates successful insertion

of the CNE into the cell and a tight seal between the electrode and the cell membrane. Only in approximately 20% of nanoelectrode insertions, extracellular species leaked inside which was concluded from an increasing $[\text{Ru}(\text{NH}_3)_6]\text{Cl}_3$ redox wave. After retraction, the voltammetric signal recovers to its initial value, excluding electrode fouling or blocking of the sensor. Each CNE can be used several times for experiments on different cells. The result demonstrates that CNEs allow probing of the intracellular space with only minimal perturbations to cellular function and viability.

As described previously,[14] the stability of H_2O_2 nanosensors crucially depends on the deposition of PB inside etched nanocavities at the tip of CNEs. Calibration curves showed a linear dependence of the cathodic current with the H_2O_2 concentration within the range $10\ \mu\text{M}$ - $3\ \text{mM}$ (Figure 2a). We employed the PB-based nanoprobe to detect endogenous H_2O_2 in murine macrophages J447A.1. Macrophages are responsible for the phagocytosis of cell debris and pathogens which they kill by an oxidative outburst,[16] i. e. the release of large amounts of ROS and RNS.

To evaluate the influence of intracellular insertion on the stability of the deposited PB film, cyclic voltammograms were recorded in PBS and inside macrophage cells (Figure 2b). The cyclic voltammogram recorded inside the cell shows largely identical voltammetric features corresponding to the oxidation/reduction of the PB/Prussian White (PW) redox couple, indicating that the intracellular environment does not substantially alter the redox properties of the PB film.

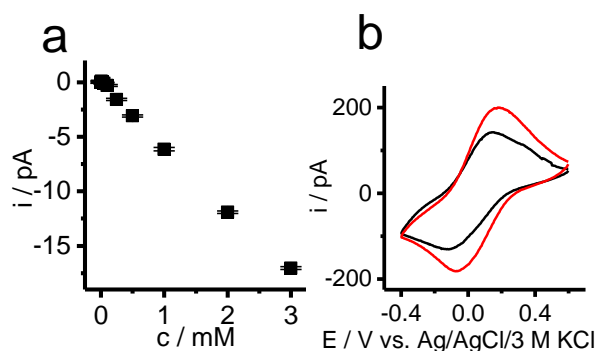


Figure 2. a: Calibration of H_2O_2 reduction currents at a PB-modified carbon nanoelectrode in $0.1\ \text{M}$ sodium phosphate buffer pH 7.0 containing $150\ \text{mM}$ KCl. b: Cyclic voltammograms of a PB-modified carbon nanoelectrode in PBS pH 7.4 (red line) and inside of a murine macrophage (black line) at $200\ \text{mVs}^{-1}$.

The working potential for penetration experiments was in the range between 0 and $-200\ \text{mV}$ vs. $\text{Ag}/\text{AgCl}/3\ \text{M}\ \text{Cl}^-$, typically at $-150\ \text{mV}$. At that potential most of the electrocatalyst layer is present in its reduced form PW, which is required for H_2O_2 reduction. As expected for PB-modified electrodes,[17] the nanosensors did not record substantial interferences caused by ascorbic acid. Interference by molecular oxygen was only observed at potentials below $-300\ \text{mV}$. To elucidate the impact of cell penetrations on cell viability and ROS production, PB-modified nanoprobe were inserted in macrophage cells without any specific stimulation of their ROS secretion. Optical micrographs of a macrophage with a PB-modified CNE inserted and after retraction (Figure 3a) show that the cell maintains its shape, indicating that penetration with a CNE does not impact cell viability.

After successful penetration of the membrane, typically a cathodic current spike is observed in the corresponding chronoamperometric data (Figure 3b), followed by a slow equilibration back to the initial current value measured in the surrounding buffer.

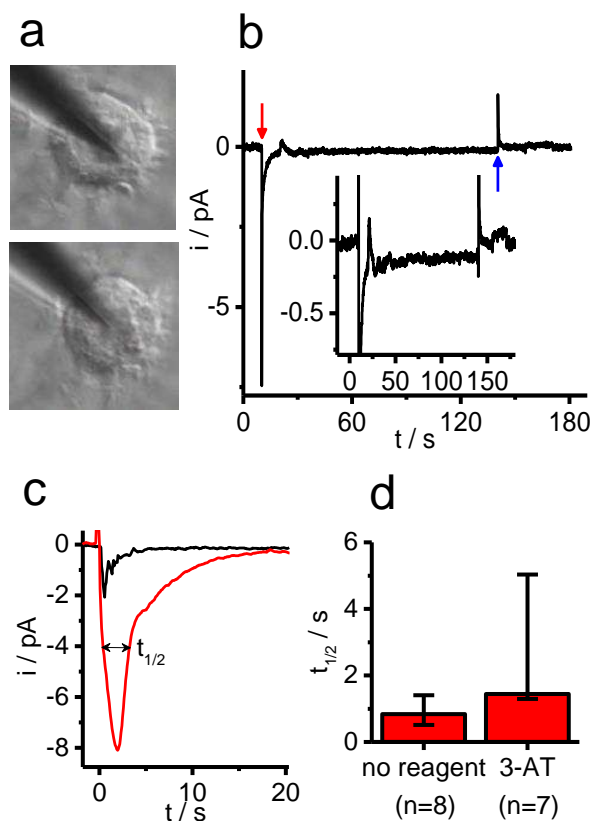


Figure 3. a: Optical micrographs of a PB-modified carbon nanoelectrode inserted into a murine macrophage (top) and after retraction (bottom). b: Typical current-time trace during a cell penetration experiment. The moment of penetration and retraction are marked with a red and blue arrow, respectively. Inset: Magnification of the same current transient. c: Comparison of the current responses for untreated cells (black) and after addition of 20 mM 3-AT to inhibit catalase (red) d: Comparison of cathodic peak half-life between catalase-inhibited and non-treated cells. Column heights represent the median whereas whiskers show the 25th and 75th percentiles.

The sharp cathodic current spikes are likely due to oxidative outbursts induced by the insertion of the nanosensor. Similar behavior has been described previously as being caused by mechanical stimulation.[9,10] As a control experiment, bare CNEs without the modification with PB were inserted into cells and no current signals were observed upon penetration. A number of ROS scavenging systems are in place to protect the cell from a detrimental overabundance of ROS. For instance, catalase accelerates the disproportionation of H₂O₂. Consequently, deactivating catalase by its inhibitor amino-1,2,4-triazole (3 AT)[18] leads to an accumulation of H₂O₂ in the cell.[19] The high temporal resolution of the nanosensors allows to monitor the course of intracellular H₂O₂ levels after an oxidative outburst. After addition of 3-AT to the cell medium, the decay of the cathodic peak observed upon cell penetration is retarded (Figure 3c) and the corresponding peak half-lives are substantially longer (Figure 3d). This behaviour is attributed to the cell's diminished capability to decompose H₂O₂ when its antioxidative protection is partially dysfunctional.

Moreover, PB-modified nanosensors are suitable to quantify the intracellular H₂O₂ level. The cell membrane is permeable to H₂O₂. [1] To mimic a situation of oxidative stress and to study the uptake of H₂O₂ from the extracellular environment into macrophage cells, a known high concentration of H₂O₂ was added to the surrounding buffer after inserting a nanosensor into

the cell (Figure 4a). Subsequently, an increase of the intracellular cathodic current is observed due to H₂O₂ crossing the cell membrane. The stable current plateau recorded a few seconds after the addition of H₂O₂ corresponds to a steady-state hydrogen peroxide concentration which is a result of the competition between permeation through the membrane and scavenging of H₂O₂ by the cell's antioxidative protection.[3] Upon retraction of the sensor, the cathodic current increases even further due to the higher extracellular H₂O₂ level.

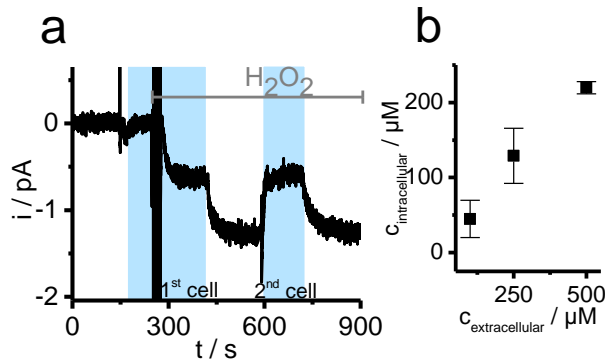


Figure 4. a: Current-time trace of penetration experiments at two distinct macrophages upon addition of H₂O₂ to the external solution to a concentration of 500 μM . A potential of -150 mV vs. Ag/AgCl/3 M KCl was applied. The blue panels indicate the periods during which the sensor was inserted into the cells. b: Intracellular H₂O₂ concentration in dependence of the concentration in the extracellular buffer. $n = 3$.

When varying the extracellular hydrogen peroxide concentration, the driving force for diffusive H₂O₂ transport across the cell membrane into the cell is modulated, resulting in a higher influx of hydrogen peroxide across the cell membrane. Consequently, the intracellular concentration scales with the extracellular H₂O₂ level (Figure 4b). This finding represents a situation of oxidative stress where the antioxidative protection cannot compete with the high influx of H₂O₂.

Conclusions

Selective electrochemical quantification of ROS species inside cells has remained challenging due to the large sensor size and a lack of specificity for the detection. We have previously reported on amperometric nanosensors for H₂O₂ detection which are fabricated by depositing Prussian Blue into etched cavities on the tip of carbon nanoelectrodes and predicted their use for the quantification of ROS species in cells.[14] We demonstrate their exploitation for selective intracellular quantification of H₂O₂. These nanoprobe are suitable to probe the intracellular environment without causing a leakage between the extra- and intracellular medium. The sensors were successfully applied for the detection of H₂O₂ during penetration-induced oxidative outbursts in murine macrophages. The temporal evolution of the transient intracellular hydrogen peroxide levels can be resolved and may be used to evaluate the antioxidative capabilities of cells. Besides, it is possible to quantify the intracellular H₂O₂ level and monitor its permeation through the cell membrane. The described experiments demonstrate that the PB-modified nanoprobe are a versatile tool to investigate the intricate balance between production, annihilation and secretion of ROS at the single-cell level. In future applications, the nanosensor could help to monitor the evolution of H₂O₂ concentration in individual cells to elucidate the role of ROS in

physiological and disease processes. The approach presented in this paper is a step towards the analysis of cells on an individual non-statistical basis which is the next big frontier in biology.[20]

Experimental Section

The preparation of carbon nanoelectrodes was described in detail elsewhere. [11,13] Briefly, quartz capillaries (Sutter Instruments) with an inner diameter of 0.9 mm and an outer diameter of 1.2 mm were pulled to nanopipettes using a P-2000 laser puller (Sutter Instruments). Typical parameters were Heat 680, Filament 4, Velocity 45, Delay 130 and Pull 120. The formed nanopipettes were connected to a butane/propane (80:20) gas container (Campingaz) and inserted into a second quartz capillary which was under low argon flow. To deposit pyrolytic carbon the nanopipette was heated with a jet torch for approximately 20 s and allowed to cool down under the inert argon atmosphere for another 10 s. The size and quality of the resulting CNEs was estimated from their diffusion-limited steady-state current in 5 mM $[\text{Ru}(\text{NH}_3)_6]\text{Cl}_3$, 0.1 M KCl solution according to the equation for disk-shaped microelectrodes $i_{ss} = 4.64 nFCDr$. Electrochemical measurements were carried out at room temperature using a two-electrode system with a Ag/AgCl pseudo-counter/reference electrode. All potentials were reported with respect to this electrode. Solutions were prepared with ultrapure water (SG). For etching the CNEs a VA-10 potentiostat (npi) was employed whereas for all other recordings an Axopatch 200B Patch Clamp amplifier (Axon Instruments) was employed. Modification of the prepared CNEs with Prussian Blue was carried out according to a procedure described elsewhere[14] with some minor modifications: For PB deposition 0.6 V were applied to the etched nanotip and it was dipped into a solution of 1 mM $\text{K}_3[\text{Fe}(\text{CN})_6]$, 1 mM FeCl_3 , 0.1 M KCl and 0.1 M HCl. After 5 min, it was cycled typically 50 times from 0.6 V to 0.3 V (100 mV/s). The activation was done in 0.1 M KCl, 0.1 M HCl by scanning from 0.6 V to 0.4 V for usually 20 to 40 cycles (200 mV/s). The murine macrophage J774A.1 (American Type Culture Collection) and the human embryonic kidney tsA201 (Sigma-Aldrich) cell lines were cultured in Dulbecco's modified Eagle's medium (DMEM) (Sigma-Aldrich) supplemented with 4500 mg/L glucose, L-glutamine, sodium bicarbonate, sodium pyruvate, 10 % foetal bovine serum and penicillin/streptomycin at 37 °C under a humidified atmosphere containing 5% CO_2 . Penetration experiments were carried out at room temperature in PBS pH 7.4 on the stage of an inverted microscope (Axiovert 25C, Zeiss) inside of a Faraday cage. 3-AT (20 mM, Sigma-Aldrich) was added to the PBS at least 5 min before starting the measurements. To avoid vibrations, the setup was placed on a damping table (TS-140, HWL Scientific Instruments). Before measuring, the cells were washed two times with PBS to remove the DMEM. For the penetration experiments depicted in Figure 1 and 3, the nanosensor was fixed in a 45° angle with respect to the cell dish. A micromanipulator (P-853, PI) was used to change the position of the nanosensor manually until it touched the cell membrane. To penetrate, a voltage was applied to a piezoelement to induce a 2.5 5 μm movement of the nanosensor along the 45° axis with respect to the cell dish. For experiments studying the H_2O_2 uptake of macrophages, the nanosensor was fixed in a 30° angle to a MPC-325 micromanipulator (Sutter Instruments). For penetration, quick impulse-like 2 μm movements along the 30° axis were carried out with the micromanipulator. For cell penetration experiments n represents the number of tested individual cells. Every electrode was calibrated before starting a cell measurement and, if H_2O_2 concentrations were calculated, the individual sensitivities were taken into account. For the results shown in

Figure 3, no correlation between the amount of deposited PB and the duration of observed current spikes during penetration experiments was found. Experiments involving extracellular concentrations of H₂O₂ were performed in the first 30 min after H₂O₂ addition. Cell death is excluded based on the cell morphology as observed in the optical microscope.

Acknowledgements

The authors are grateful for financial support by the Deutsch-Israelische Projektkooperation in the framework of the project “Nanoengineered optoelectronics with biomaterials and bioinspired assemblies” and the Cluster of Excellence RESOLV (EXC 1069) funded by the Deutsche Forschungsgemeinschaft (DFG). An automatic micromanipulator was generously provided by Dr. Patrick Happel.

Keywords: biosensors • hydrogen peroxide detection • nanoelectrode • reactive oxygen species • single-cell analysis

- [1] J. R. Stone, S. Yang, *Antioxid. Redox Sign.* 2006, 8, 243–270.
- [2] a) G. Waris, H. Ahsan, *J. Carcinog.* 2006, 5; 14. b) D. A. Patten, M. Germain, M. A. Kelly, R. S. Slack, *J. Alzheimers Dis.* 2010, 20, 357–367; c) M. Valko, D. Leibfritz, J. Moncol, Cronin, Mark T. D., M. Mazur, J. Telser, *Int. J. Biochem. Cell Biol.* 2007, 39, 44–84.
- [3] T. Finkel, N. J. Holbrook, *Nature* 2000, 408, 239–247.
- [4] S. I. Dikalov, D. G. Harrison, *Antioxid. Redox Sign.* 2014, 20, 372–382.
- [5] a) S. Dikalov, K. K. Griendling, D. G. Harrison, *Hypertension* 2007, 49, 717–727; b) B. Kalyanaraman, V. Darley-Usmar, Davies, Kelvin J. A., P. A. Dennery, H. J. Forman, M. B. Grisham, G. E. Mann, K. Moore, Roberts II, L. Jackson, H. Ischiropoulos, *Free Radic. Bio. Med.* 2012, 52, 1–8; c) G. Bartosz, *Clin. Chim. Acta* 2006, 368, 53–76.
- [6] a) N. V. Kulagina, A. C. Michael, *Anal. Chem.* 2003, 75, 4875–4881; b) P. Salazar, M. Martín, R. D. O’Neill, R. Roche, J. L. González-Mora, *Int. J. Electrochem. Sci.* 2012, 7, 5910–5926; c) P. Salazar, M. Martín, R. Roche, R. O’Neill, J. González-Mora, *Electrochim. Acta* 2010, 55, 6476–6484; d) R. Li, X. Liu, W. Qiu, M. Zhang, *Anal. Chem.* 2016, 88, 7769–7776.
- [7] a) X. T. Zheng, W. Hu, H. Wang, H. Yang, W. Zhou, C. M. Li, *Biosens. Bioelectron.* 2011, 26, 4484–4490; b) A. Schulte, W. Schuhmann, *Angew. Chem. Int. Ed.* 2007, 46, 8760–8777; c) M. Nebel, S. Grützke, N. Diab, A. Schulte, W. Schuhmann, *Angew. Chem. Int. Ed.* 2013, 52, 6335–6338; d) J. Clausmeyer, W. Schuhmann, *Trends Anal. Chem.* 2016, 79, 46–59; e) Y. Zhang, J. Clausmeyer, B. Babakinejad, A. Lopez Cordoba, T. Ali, A. Shevchuk, Y. Takahashi, P. Novak, C. Edwards, M. Lab et al., *ACS Nano* 2016, 10, 3214–3221.
- [8] a) S. Arbault, P. Pantano, J. A. Jankowski, M. Vuillaume, C. Amatore, *Anal. Chem.* 1995, 67, 3382–3390; b) S. Arbault, P. Pantano, N. Sojic, C. Amatore, M. Best-Belpomme, A. Sarasin, M. Vuillaume, *Carcinogenesis* 1997, 18, 569–574; c) C. Amatore, S. Arbault, A. C. W. Koh, *Anal. Chem.* 2010, 82, 1411–1419.
- [9] C. Amatore, S. Arbault, C. Bouton, K. Coffi, J.-C. Drapier, H. Ghandour, Y. Tong, *ChemBioChem* 2006, 7, 653–661.
- [10] Y. Wang, J.-M. Noël, J. Velmurugan, W. Nogala, M. V. Mirkin, C. Lu, M. G. Collignon, F. Lemaître, C. Amatore, *Proc. Natl. Acad. Sci. U.S.A.* 2012, 109, 11534–11539.
- [11] Y. T. Takahashi, A. I. Shevchuck, P. Novak, Y. Zhang, N. Ebejer, J. V. Macpherson, P. R. Unwin, A. J. Pollard, D. Roy, C. A. Clifford et al., *Angew. Chem. Int. Ed.* 2011, 50, 9638–9642.
- [12] a) Y. Takahashi, A. I. Shevchuk, P. Novak, B. Babakinejad, J. Macpherson, P. R. Unwin, H. Shiku, J. Gorelik, D. Klenerman, Y. E. Korchev et al., *Proc. Natl. Acad. Sci. U.S.A.* 2012, 109,

- 11540–11545; b) K. McKelvey, B. P. Nadappuram, P. Actis, Y. Takahashi, Y. E. Korchev, T. Matsue, C. Robinson, P. R. Unwin, *Anal. Chem.* 2013, 85, 7519–7526.
- [13] P. Actis, S. Tokar, J. Clausmeyer, B. Babakinejad, S. Mikhaleva, R. Cornut, Y. T. Takahashi, A. López Córdoba, P. Novak, A. I. Shevchuck et al., *ACS Nano* 2014, 8, 875–884.
- [14] J. Clausmeyer, P. Actis, A. López Córdoba, Y. Korchev, W. Schuhmann, *Electrochem. Commun.* 2014, 40, 28–30.
- [15] P. Sun, F. O. Laforge, T. Abeyweera, S. A. Rotenberg, J. Carpino, M. V. Mirkin, *Proc. Natl. Acad. Sci. U.S.A.* 2008, 105, 443–448.
- [16] J. M. Slauch, *Mol. Microbiol.* 2011, 80, 580–583.
- [17] F. Ricci, A. Amine, G. Palleschi, D. Moscone, *Biosens. Bioelectron.* 2003, 18, 165–174.
- [18] D. Darr, I. Fridovich, *Biochem. Pharmacol.* 1986, 35, 3642.
- [19] a) J. I. Koepke, C. S. Wood, L. J. Terlecky, P. A. Walton, S. R. Terlecky, *Toxicol. Appl. Pharm.* 2008, 232, 99–108; b) S. Y. Kim, S. M. Lee, J.-W. Park, *Free Radical Res.* 2006, 40, 1190–1197.
- [20] a) R. Zenobi, *Science* 2013, 342, 1243259; b) C. Schubert, *Nature* 2011, 480, 133–137; c) J. R. Heath, A. Ribas, P. S. Mischel, *Nat. Rev. Drug Discov.* 2016, 15, 204–216.